Proceedings Paper:

Santinello, M, Colombo, M orcid.org/0000-0002-4335-4250, Cammi, A et al. (1 more author) (2017) CFD study of two-phase flow in a helical tube. In: Transactions of the American Nuclear Society. 2017 ANS Winter Meeting, 29 Oct - 02 Nov 2017, Washington, DC, USA. American Nuclear Society , pp. 1768-1771.

CFD Study of Two-phase Flow in a Helical Tube

M. Santinello[a], M. Colombo[b], A. Cammi[a], M.E. Ricotti[a]

[a] Politecnico di Milano, dept. of Energy - CeSNEF-Nuclear Engineering division, via La Masa 34, 20156 Milano, Italy
[b] School of Chemical and Process Engineering, University of Leeds, Leeds LS2 9JT, United Kingdom

marco.santinello@polimi.it, m.colombo@leeds.ac.uk, antonio.cammi@polimi.it, marco.ricotti@polimi.it

INTRODUCTION

Currently, significant research efforts are being focused on the thermal-hydraulics of the helically coiled tube, because of the improved compactness, performance and reliability this can provide to heat exchanger design. Helicoidal heat exchangers and steam generators are extensively used in industry and, in the nuclear field, in some prototypes of innovative reactor designs such as the sodium-cooled fast reactor. Nowadays, technical features of the helical pipe are mostly appealing for the compact design of integral Small Modular Reactors (SMRs), e.g. CAREM, SMART, IRIS and NuScale [1]. However, additional understanding of several phenomena occurring in helical tubes is necessary to further increase safety and efficiency during operation. Among others, heat transfer, pressure drop, free convection and flow instabilities. In particular, the profile of two-phase flow pressure drop is a key aspect for the design and optimization of the steam generator, but because of the complexity of the subject our knowledge and predictive capability is still incomplete and mainly based on empiricism.

It is known from literature that in some situations the pressure drop vs. quality profile for a vertical rectilinear pipe may exhibit a small peak near the dryout zone [2]: pressure drop due to friction increases up to the thermal crisis and then decreases with mass quality approaching unity. In helically coiled tubes, experimental data show that such peak is much more prominent and may lead to a large decrease of the pressure drop in the post-dryout zone. [3]. Responsible of this behavior is the centrifugal force field that affects the interaction of the fluid with the wall and the gas phase. Nevertheless, the physics behind such a significant discrepancy with respect to the rectilinear pipe has not been completely understood yet.

This work investigates the pressure drop for a two-phase steam-water mixture flowing inside a helically coiled tube under adiabatic conditions. A high-pressure two-phase flow is simulated using the ANSYS Fluent 15.0 Computational Fluid Dynamic (CFD) code. The specific geometry of a test section (i.e. IES facility, built and operated as SIET labs, in Italy [4]) for forced flow experiences in a helically coiled tube is modelled and two-phase flow pressure drop measurements [3] are used to validate the CFD results. Once validated, wall shear stress profiles available from the CFD are analyzed to provide a physical interpretation for the peak in the pressure drop profile.

DESCRIPTION OF THE WORK

Overview

Nowadays, the application of two-phase flow CFD to thermal hydraulic issues has become increasingly common in nuclear reactor research [5]. However, due to the significant modeling complexities, publications available for two-phase flow in helical tubes are rather limited and most of them regards an air-water mixture [6-8]. In these works, and also in those where the steam-water flow is simulated [9-10], an Eulerian-like multi-phase approach is often preferred. In this work, the two-phase steam-water flow inside a small portion of the IES test section helical tube is resolved. Main geometrical parameters of the test section are listed in Table I. Simulations assume adiabatic conditions and a steam-water mixture at the inlet of the tube. Exact experimental conditions, which were obtained by evaporating the water inside a pre-heater while maintaining the test section in adiabatic conditions, are recreated. More specifically, ten cases were simulated that cover the entire range of mass quality from 0.01 to 0.93 (Table II.).

Table I. Geometrical features of IES test section

Inner tube diameter (m)	12.53e-3
Coil diameter (m)	1.0
Tube length (m)	32.0
Test section height (m)	8.0

Table II. List of inlet mass quality for the ten simulations

0.01	0.15	0.25	0.38	0.50	0.59	0.67	0.78	0.85	0.93

Governing Equations of the CFD Model

The CFD model is based on the Eulerian – Eulerian two-fluid approach. After averaging, both phases becomes interpenetrating continua that are allowed to co-exist at any point with the relative weight between liquid and vapor quantified by the void fraction. Such approach does not allow resolving the detailed topology of the two phases. Interfacial transfers are entirely modelled with opportune closure laws that are mainly based on correlations with the average flow conditions. Since experimental pressure drop measures have been taken in adiabatic conditions, there is no need to solve the energy equation and the two fluids are assumed in thermal equilibrium at the saturation temperature.

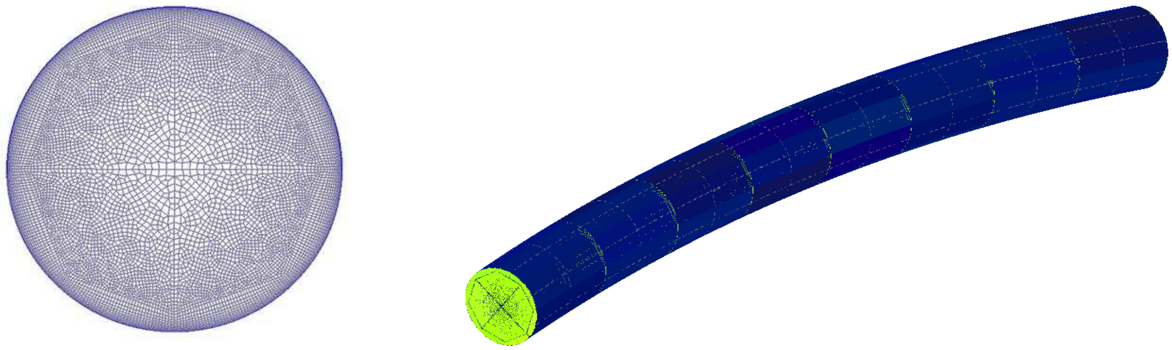

Fig. 1 Cross section and 3D view of the mesh

For the same reason, and because of the small length of the geometry considered, constant thermo-physical properties are also assumed. For the n^{th} phase, the governing equations solved by the code are:

$$\frac{\partial}{\partial t}(\alpha_n \rho_n) + \nabla \cdot (\alpha_n \rho_n \overline{V_n}) = 0 \quad (1)$$

$$\frac{\partial}{\partial t}(\alpha_n \rho_n \overline{V_n}) + \nabla \cdot (\alpha_n \rho_n \overline{V_n V_n}) = \\ = -\alpha_n \nabla p + \nabla \cdot \overline{\overline{\tau_n}} + \alpha_n \rho_n \overline{g} + \sum_{p=1}^{2} \overline{M_{pn}} \quad (2)$$

The momentum exchange between the phases M_{pn} is assumed to be due only to the drag force and other interfacial force terms are neglected. Drag model is based on the dispersed phase approach proposed by Kolev [11]. In this method, a critical aspect is the size of the bubble/droplet. This has turned out to be a very sensitive parameter, whose impact has been carefully analyzed in Colombo et al. [7]. It has been optimized to 0.1 mm, after having observed that lower values generate convergence problems and higher values originates a weaker interaction between the two-phases.

Turbulence is modeled with the k-ε model. The near wall behavior is resolved with the wall law proposed by Kader [12]. Validity of this model extends over the entire wall region by blending the linear $u^+ - y^+$ relation in the viscous sublayer with the logarithmic law of the wall in the fully-turbulent region. The pressure-velocity coupling is resolved using the Phase Coupled SIMPLE scheme. Momentum and turbulent quantities are discretized with the second order upwind scheme, while the QUICK scheme is used for the void fraction. Simulations are time-dependent and the time step is determined in such a way that the Courant number limit is always respected.

Domain and Mesh

The domain considered for the simulations is a 15cm-long section of the helical tube. The mesh is composed by over 2.7 million elementary volumes. The average density is 168,994 volumes/cm^3. The cross section is subdivided into 10,560 cells (Fig. 1). The mesh near the wall is structured and gradually refined approaching the wall. The central part is instead unstructured and coarser. The wall treatment adopted in the CFD model allows a fine boundary layer, but does not require a very low y^+ value in the nearest wall cell. This is an important feature to control the number of elements and the computational load, since the flow velocity of cases around the dry-out point determine a quite high y^+. Main mesh quality parameters are shown in Table III.

Table III. Mesh quality parameters

Width of nearest wall cell (m)	1.33e-5
Max Skewness	0.36
Max Orthogonal Quality	0.64

Boundary Conditions

Due to the limited length of the domain considered, fully-developed flow conditions were imposed at the pipe inlet. These conditions were obtained from a set of preliminary simulations with a coarser mesh but of a longer section of the pipe. The preliminary simulations use homogeneous flow at the inlet. The coarser mesh reproduces a 3.14m-long helical tube (equal to one round of the IES test section), and has a density of 4,274 volumes/cm^3.

The inlet velocity varies from 0.68 to 18.56 m/s, depending on the flow quality, to exactly match the measured mass flux of the experimental data, i.e. 389 kg/m^2s. Fixed pressure is imposed on the outlet surface. Constant fluid properties are assumed and these are calculated at 3.8 MPa saturation point for both liquid and gas, i.e. the conditions of the experiments. At the wall, non-slip and adiabatic conditions are assumed.

RESULTS

Pressure Drop

Numerical predictions of the frictional pressure drop show qualitative and quantitative agreement with the experimental data (Fig. 2). CFD is able to successfully reproduce the peak of the profile around the dry-out zone. The maximum deviation from the experiments is about 25%, for the case x = 0.38, whereas the average deviation is 8.5%.

The best adherence between simulations and experiments is observed for low ($x \leq 0.25$) and high ($x \geq 0.85$) steam quality, these being closer to single-phase flow conditions The satisfactory results allow concluding that the CFD model here presented is able to predict pressure drop in a helically coiled tube with accuracy, even in the relatively high pressure conditions considered.

The maximum y^+ of the calculations varies between 3.43 and 24.00, for x = 0.01 and x = 0.78 respectively. Grid sensitivity has been evaluated comparing pressure drop predictions with those given by coarser meshes. Small discrepancies with respect to the reference case have been found, showing that the simulations are not sensitive to the discretization of the domain.

Void fraction

The void fraction distribution in the pipe cross-section is shown in Fig. 3. The centrifugal force shows its effect mainly in the central range of the quality spectrum. With very low steam quality (x = 0.01), the effect of gravity is still predominant. At higher quality, x = 0.15-0.67, fluid velocity is also higher and the centrifugal force begins to affect the phase distribution, leading the liquid to accumulate near the wall in the lower-outer portion of the pipe. A liquid film starts to appear at the wall, although it is not completely resolved by the code, and remains visible up to x = 0.78. The flow cannot strictly be considered an annular regime as in a vertical rectilinear duct: because of the centrifugal force, the thickness of the film is not constant along the wall. At even higher void, the flow regime resembles a dispersed flow, even though the near wall region is still characterized by a lower void fraction, therefore by a higher liquid content

Analysis of wall shear stress profiles

The transition from the annular-like regime to the dispersed flow, caused by the gradual depletion of the liquid film around the wall, occurs near the peak in the pressure drop profile and can provide an explanation for this behavior. Values of the liquid and the vapor components of the wall shear stress are available from the code and are plotted in Fig. 4. The liquid-phase component plays the key role in the total wall shear stress value, especially before the transition to a dispersed flow regime. The maximum of the liquid contribution corresponds to the liquid build-up region in the lower – outer portion of the pipe. As much as the flow velocity increase, so does the radial velocity gradient in the near-wall zone, where the liquid phase accumulates. The presence of the centrifugal force breaks the symmetry of the liquid film in the annular flow region. This results in a higher wall shear stress, with respect to a rectilinear duct, due to the presence of the build-up. After the liquid has depleted, the wall shear stress relaxes and, consequently, pressure drop decreases. Such behavior provides a physical interpretation for the peak in the pressure drop profile.

This work can have important implications for the study of the two-phase flow in the helically coiled tube, suggesting innovative approaches for the determination of pressure drop correlations. In addition, it also show the good capability of the Eluerian model to predict the experimental data. Further verifications might be obtained with interface-tracking methods, which aim at resolving the position of the interface.

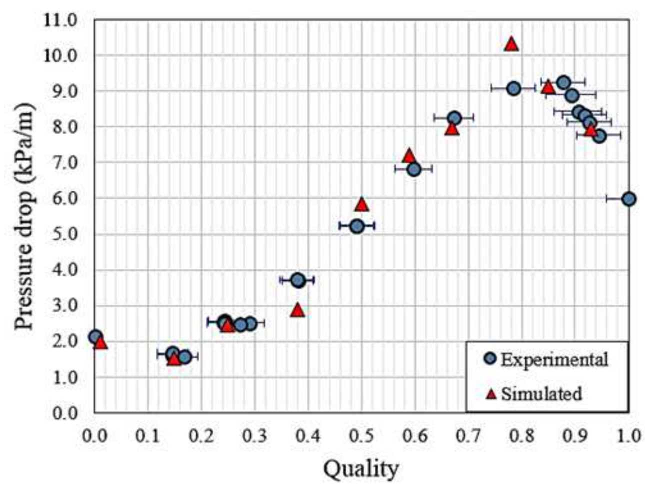

Fig. 2 Comparison between experimental and predicted pressure drop (experimental error on Δp is ±0.4%).

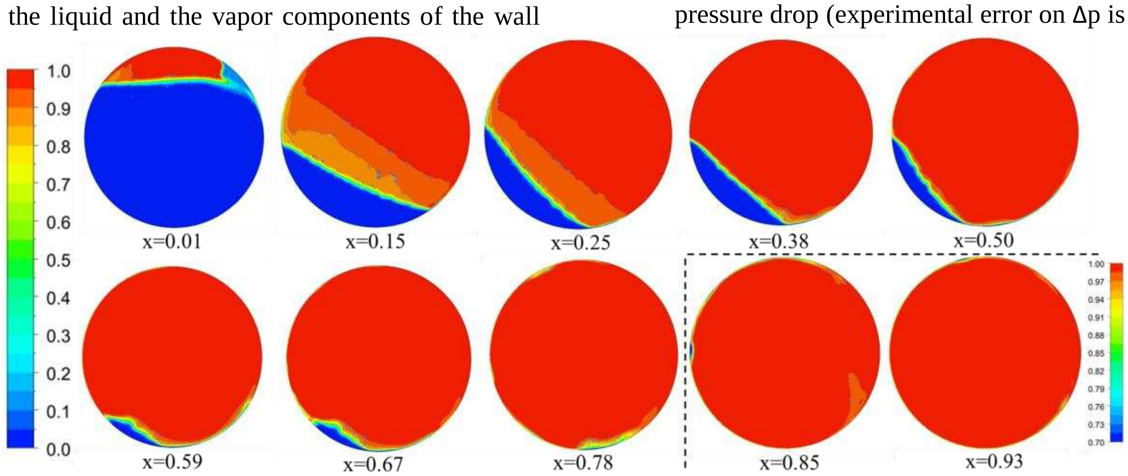

Fig. 3 Void fraction profiles in the tube. The outer part of the coil is at nine o'clock.

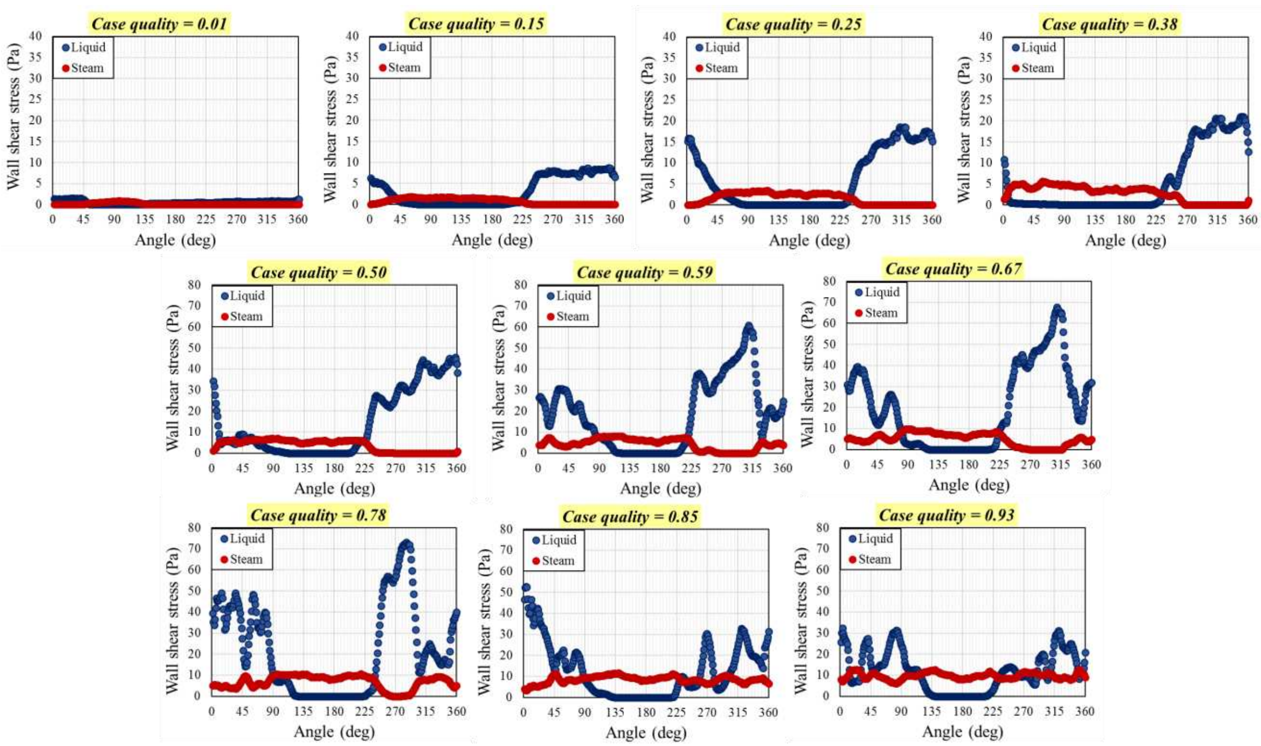

Fig. 4 Wall shear stress profiles: 0° is the outer part of the tube (nine o'clock in Fig. 3) and clockwise convention is used

NOMENCLATURE

g = gravity constant	x = mass quality
p = pressure	α = volume fraction
t = time	ρ = density
V = velocity	$\bar{\bar{\tau}}$ = stress tensor

REFRENCES

1. IAEA, "Advances in Small Modular Reactor Technology Development - A Supplement to: IAEA Advanced Reactors Information System (ARIS)", International Atomic Energy Agency (2016).
2. G. P. GASPARI, C. LOMBARDI, G. PETERLONGO, "Pressure Drops in Steam-Water Mixtures. Round Tubes--Vertical Upflow", CISE (1964).
3. M. COLOMBO, L.P.M. COLOMBO, A. CAMMI, M.E. RICOTTI, "A scheme of correlation for frictional pressure drop in steam–water two-phase flow in helicoidal tubes", Chem. Eng. Sci., **123**, 460-473 (2015).
4. L. SANTINI, A. CIONCOLINI, C. LOMBARDI, M.E. RICOTTI, "Two-phase pressure drops in a helically coiled steam generator" Int. J. Heat Mass Tran., **51,** 4926-4939 (2008).
5. D. BESTION, "Applicability of Two-Phase CFD to Nuclear Reactor Thermal-Hydraulics and Elaboration of Best Practice Guidelines", Nucl. Eng. Des., **253**, 311-321 (2012).
6. J.S. JAYAKUMAR, S.M. MAHAJANI, J.C. MANDAL, K.N. IYER, P.K. VIJAYAN, "Thermal Hydraulic Characteristics of Air-Water Two-Phase Flows in Helical Pipes", Chem. Eng. Res. Des., **88**, 501-512 (2010).
7. M. COLOMBO, A. CAMMI, G.R. GUEDON, F. INZOLI, M.E. RICOTTI "CFD Study of an Air-Water Flow Inside Helically Coiled Pipes", Prog. Nucl. Energy, **85,** 462–472 (2015).
8. X LIU, D ZHAO, Y LIU, S JIANG, H XIANG, "Numerical Analysis of the Two-Phase Flow Characteristics in Vertical Downward Helical Pipe", Int. J. Heat Mass Tran, **108,** 1947-1959 (2017).
9. J.C. JO, W.S. KIM, C.Y. CHOI, Y.K. LEE, "Numerical Simulation of Subcooled Flow Boiling Heat Transfer in Helical Tubes", ASME J. Pres. Ves. Tech., **131**, (2009).
10. T.T. CHANDRATILLEKE, N. NADIM, R. NARAYANASWAMY, "An Investigation of Flow Boiling with Secondary Flow Interaction in Curved Pipes", ECI 8th Int. Conf. Boiling Cond. Heat Tran., Lausanne, Switzerland, June 3-7, 2012, World Scientific (2012).
11. N.I. KOLEV, "Multiphase Flow Dynamics 2: Thermal and Mechanical Interactions". Springer, Berlin, Germany, 3nd Edition (2007).
12. B. KADER. "Temperature and Concentration Profiles in Fully Turbulent Boundary Layers". Int. J. Heat Mass Transfer, **24,** 1541–1544 (1981).